

Fracture toughness of polycrystalline silicon carbide thin films

J. J. Bellante and H. Kahn

Department of Materials Science and Engineering, Case Western Reserve University, Cleveland, Ohio 44106

R. Ballarini

Department of Civil Engineering, Case Western Reserve University, Cleveland, Ohio 44106

C. A. Zorman and M. Mehregany

Department of Electrical Engineering and Computer Science, Case Western Reserve University, Cleveland, Ohio 44106

A. H. Heuer

Department of Materials Science and Engineering, Case Western Reserve University, Cleveland, Ohio 44106

(Received 13 August 2004; accepted 16 December 2004; published online 11 February 2005)

Thin film polycrystalline silicon carbide (poly-SiC) doubly clamped microtensile specimens were fabricated using standard micromachining processes, and precracked using microindentation. The poly-SiC had been deposited on Si wafers by atmospheric pressure chemical vapor deposition, a process which leads to residual tensile stresses in the poly-SiC thin films; we measured the residual stress adjacent each specimen via a micromachined strain gauge. The stress intensity factor, K_I , at the crack tip in each specimen depends on the magnitude of these residual stresses and the precrack length. Upon release, those precracks whose stress intensity exceeded a critical value, K_{Ic} , propagated to failure, whereas no crack growth was observed in those precracks with $K < K_{Ic}$. The fracture toughness so determined was $2.8 \leq K_{Ic} \leq 3.4 \text{ MPa m}^{1/2}$. Our technique also allowed us to assess any susceptibility to moisture-assisted stress corrosion cracking, which proved to be essentially absent in poly-SiC. © 2005 American Institute of Physics. [DOI: 10.1063/1.1864246]

SiC devices are attractive for use in high power, high frequency electronic applications, due to their high thermal conductivity, high breakdown field, and high electron saturation velocity.¹ Furthermore, SiC is a promising candidate for high temperature, harsh environment applications for microelectromechanical systems (MEMS) because of SiC's superior mechanical and tribological properties compared to silicon used in more conventional components. Several SiC MEMS devices have been reported, including pressure sensors,^{2,3} bolometers,⁴ resonators,^{5,6} and fuel atomizers;⁷ these were fabricated from either amorphous^{3,4} or cubic (referred to as 3C or β)^{2,5-7} SiC, due to the relative ease of fabrication of these forms of SiC thin films via atmospheric or low pressure chemical vapor deposition (APCVD and LPCVD, respectively).

Knowledge of the mechanical behavior of SiC is necessary for reliable design of efficient, high performance, long lifetime devices. In particular, intrinsic materials properties that are independent of specimen geometry, such as the fracture toughness, K_{Ic} , and possible susceptibility to stress corrosion cracking are critical for device and application engineering.

Unfortunately, previous data on these properties have not been conclusive. K_{Ic} values for bulk CVD polycrystalline SiC (poly-SiC)⁸⁻¹³ have varied from 0.78 to 3.4 $\text{MPa m}^{1/2}$, as measured by indentation tests,^{8-10,12} bend tests,¹¹ and double cantilever tests.¹² Stress corrosion cracking, also referred to as static fatigue or environmentally assisted crack growth in the ceramics literature, has been demonstrated in numerous ceramic materials, most notably SiO_2 where moisture is the corrosive agent.¹⁴ Stress corrosion cracking in CVD SiC has not been studied, but crack growth has been

studied in sintered and hot-pressed SiC^{15,16} but exhibited no dependence on environment.

To determine K_{Ic} and to assess possible stress corrosion cracking in APCVD SiC on a scale relevant to MEMS, we fabricated the doubly clamped single edge-cracked beams shown in Fig. 1. These devices exploit residual tensile stresses to load precracks and have previously been used to determine K_{Ic} of polycrystalline silicon.¹⁷ In this investigation, the microtensile devices were formed from poly-SiC,

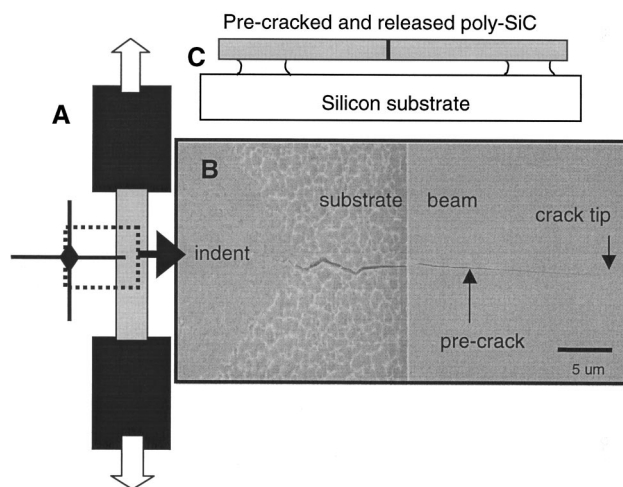


FIG. 1. (a) Schematic of $500 \mu\text{m} \times 60 \mu\text{m}$ fixed grip microtensile specimen and the location of the indent. The black rectangles represent the beam anchor pads; (b) SEM micrograph of the indent in the silicon substrate and microcrack propagation into the poly-SiC beam; (c) schematic of the pre-cracked, released poly-SiC specimen suspended above and anchored to the silicon substrate.

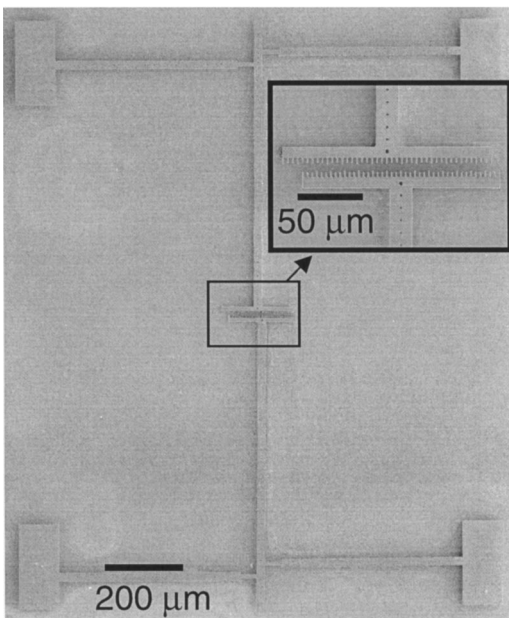


FIG. 2. Scanning electron micrograph of a poly-SiC microstrain gauge used to measure residual stress and strain. The inset shows a higher magnification micrograph of the verniers after release, indicating a residual tensile strain of 0.038% (residual tensile stress of 150 MPa).

using the following fabrication sequence: (i) a 2.8 μm thick 3C poly-SiC film with an average grain size of 25 nm was deposited onto a 100 mm diameter (100) Si wafer via APCVD using SiH_4 , C_3H_8 , and H_2 at 1050 $^\circ\text{C}$;¹⁸ (ii) a Ni masking layer was sputter deposited; (iii) standard photolithography was used to pattern the devices in photoresist; (iv) the Ni mask was wet-chemically etched, and the poly-SiC was reactively ion etched using CHF_3 , O_2 , and He; and (v) the Ni mask was removed by wet etching and the substrate was indented using a Vickers microindenter with a 1 kg load.

As shown in Fig. 1, the radial crack that had formed at the corner of indents placed $\sim 30 \mu\text{m}$ from the edge of the beam in the Si substrate propagated through the Si substrate into the overlying poly-SiC film, thus generating a precrack in the beam. The precrack length was measured using high-resolution scanning electron microscopy (SEM). Due to the stochastic nature of indent-induced cracks and the variation in the distance from the center of the indent to the edge of the beam, the precrack length varied significantly among different beams.

Before release, the 100 mm wafer was sectioned into 1 cm^2 dice, each containing 12 poly-SiC microtensile devices. Due to the vagaries of our CVD reactor, the residual stress of the poly-SiC film varied across the wafer, although room temperature stresses were consistently tensile due to the thermal expansion mismatch with the Si substrate. Therefore, the local stress in the poly-SiC device in each die was measured using microstrain gauges fabricated adjacent to the tensile beams.¹⁷ Figure 2 shows a micrograph of a poly-SiC strain gauge; upon release of the device, the sign and magnitude of the displacement of the verniers at the ends of the long suspended beams allows the residual stress to be determined with a 2 MPa uncertainty. Young's modulus of the poly-SiC on each die was also determined using lateral resonant devices.¹⁹

The beams were released by etching away the underlying Si using a 1:2:2 aqueous solution of

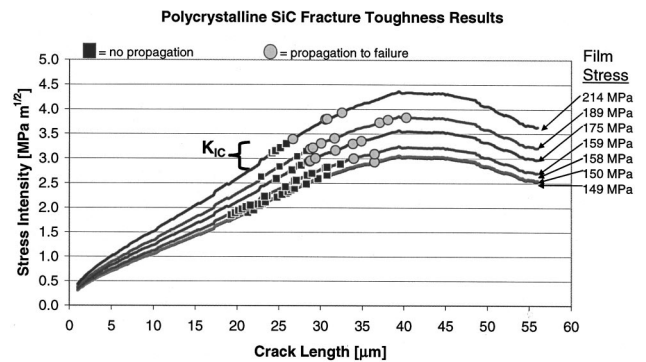


FIG. 3. Stress intensity factor, K , calculated using finite elements plotted vs crack length, with data shown as circles or filled squares.

$\text{HF}:\text{HNO}_3:\text{CH}_3\text{COOH}$. Due to the large lateral dimensions of the anchor pads at both ends of the beam, these pads remained attached to the Si substrate after the beam was fully released. Upon release, the residual tensile stress in each doubly clamped poly-SiC microtensile specimen produced a well-defined stress intensity at the crack tip. The variation in crack lengths from specimen to specimen and the associated variation in the stress required to maintain the fixed displacement conditions at the ends of the specimens produced a range of K 's at the crack tips, which were calculated through finite element analysis.²⁰ The determination of residual stress and stress intensity both depend on Young's modulus; the average value obtained by the lateral resonant devices, 393 GPa, is consistent with previous data on APCVD SiC films.^{6,8,21,22}

Seven dice were studied; the average residual stress of the poly-SiC on these dice varied from 149 to 214 MPa. The stress intensity factor for each die is shown as a function of precrack length in Fig. 3, which also displays the results of testing 73 specimens from these different dice. The fracture toughness, K_{Ic} , was bounded by the range between the lowest K that resulted in crack propagation and the highest K that did not. There is some scatter in the results from devices with different residual stresses, but taken as a whole, the data indicate that $2.8 \leq K_{Ic} \leq 3.4 \text{ MPa m}^{1/2}$. The scatter in the data is attributed mainly to the uncertainty in the film stress measurements¹⁷ and the possibility that the crack front is inclined to the film normal, as the experiment is otherwise both rigorous and straightforward. (We note that poly-SiC satisfies the demands of linear elastic fracture mechanics,²³ i.e., it is a perfectly brittle material at room temperature with atomically sharp crack tips.) For comparison, K_{Ic} for polysilicon determined using the same technique is $0.81 \pm 0.05 \text{ MPa m}^{1/2}$.¹⁷

Following the fracture toughness experiments, a total of 24 beams with precracks that had not propagated and were loaded by residual tensile stresses of 150, 159, or 214 MPa were placed in a chamber at 90% relative humidity. The residual tensile stresses induced a range of stress intensities from 1.94 to 3.30 $\text{MPa m}^{1/2}$ at the crack tips, just at or below K_{Ic} . Thus, if the moist environment induced any subcritical crack growth, the cracks would eventually reach a critical length and propagate to failure. The microspecimens were held in this humid ambient for 30 days, but no crack growth was observed. The absence of crack growth in these specimens indicates that silicon carbide is not susceptible to moisture-induced static stress-corrosion cracking. (Given the

uncertainty in crack length measurement following the 30 day exposure to a moist ambient, the maximum crack growth rate that could have occurred in the experiment was 3.9×10^{-14} m/s.) This is similar to the case of polysilicon, where conventional stress corrosion cracking is also absent.¹⁷

In summary, poly-SiC single edge-cracked doubly clamped specimens were fabricated using processes and size scales relevant to MEMS devices. Atomically sharp pre-cracks were introduced via microindentation, and the stress intensity at each crack tip was determined from an independent measure of the residual stress. The fracture toughness of poly-SiC was $2.8 \leq K_{Ic} \leq 3.4$ MPa m^{1/2}. Twenty four pre-cracked specimens with stress intensities just at or below K_{Ic} displayed no stress corrosion-induced subcritical crack growth after 30 days at 90% relative humidity.

¹G. L. Harris, *Properties of silicon carbide* (The Institute of Electrical Engineers, London, 1995).

²C. Gourbeyre, T. Chassagne, M. Le Berre, G. Ferro, E. Gautier, Y. Monteil, and D. Barbier, *Sens. Actuators, A* **99**, 31 (2002).

³A. F. Flannery, N. J. Mourlas, C. W. Storment, S. Tsai, S. H. Tan, J. Heck, D. Monk, T. Kim, B. Gogoi, and G. T. A. Kovaks, *Sens. Actuators, A* **70**, 48 (1998).

⁴A. Klumpp, U. Schaber, H. L. Offereins, K. Kuhl, and H. Sandemaier, *Sens. Actuators, A* **41–42**, 310 (1994).

⁵Y. T. Tang, K. L. Ekinci, X. M. Huang, L. M. Schiavone, M. L. Roukes, C. A. Zorman, and M. Mehregany, *Appl. Phys. Lett.* **78**, 162 (2001).

⁶S. Roy, R. G. DeAnna, C. A. Zorman, and M. Mehregany, *IEEE Trans.*

Electron Devices **49**, 2323 (2002).

⁷N. Rajan, M. Mehregany, C. A. Zorman, S. Stefanescu, and T. P. Kicher, *J. Microelectromech. Syst.* **8**, 251 (1999).

⁸X. Li, B. Bhushan, *Thin Solid Films* **340**, 210 (1999).

⁹H. Wang, R. N. Singh, and J. S. Goela, *J. Am. Ceram. Soc.* **78**, 2437 (1995).

¹⁰M. C. Osborne, J. C. Hay, L. L. Snead, and D. Steiner, *J. Am. Ceram. Soc.* **82**, 2490 (1999).

¹¹F. C. Chen and A. J. Ardell, *Mater. Res. Innovations* **3**, 250 (2000).

¹²K. Niihara, *Ceram. Bull.* **63**, 1160 (1984).

¹³J. S. Goela and M. A. Pickering, *Ceram. Eng. Sci. Proc.* **19**, 579 (1998).

¹⁴S. M. Wiederhorn and L. H. Boltz, *Am. Ceram. Soc. Bull.* **53**, 336543 (1970).

¹⁵A. G. Evans and F. F. Lange, *J. Mater. Sci.* **10**, 1659 (1975).

¹⁶K. D. McHenry, T. Yonushonis, and R. E. Tressler, *J. Am. Ceram. Soc.* **59**, 262 (1976).

¹⁷H. Kahn, R. Ballarini, J. J. Bellante, and A. H. Heuer, *Science* **298**, 1215 (2002).

¹⁸A. A. Yasseen, C. A. Zorman, and M. Mehregany, *J. Microelectromech. Syst.* **8**, 237 (1999).

¹⁹W. C. Tang, T.-C. H. Nguyen, and R. T. Howe, *Sens. Actuators* **20**, 25 (1989).

²⁰The finite element code FRANC2D was used to determine stress intensities. This code is available from the Cornell Fracture Group at <http://www.cfg.cornell.edu/>

²¹J. S. Mitchell, Masters thesis, Case Western Reserve University, 2000.

²²M. Mehregany, L. Tong, L. G. Matus, and D. J. Larkin, *IEEE Trans. Electron Devices* **44**, 74 (1997).

²³B. R. Lawn, B. J. Hockey, and S. M. Wiederhorn, *J. Mater. Sci.* **15**, 1207 (1980).